The physics of a model colloid–polymer mixture

2002 J. Phys.: Condens. Matter 14 R859

(http://iopscience.iop.org/0953-8984/14/33/201)

INSTITUTE OF PHYSICS PUBLISHING JOURNAL OF PHYSICS: CONDENSED MATTER

J. Phys.: Condens. Matter **14** (2002) R859–R880 PII: S0953-8984(02)38822-2

TOPICAL REVIEW

The physics of a model colloid–polymer mixture

W C K Poon

Department of Physics and Astronomy, The University of Edinburgh, Mayfield Road, Edinburgh EH9 3JZ, UK

Received 1 July 2002
Published 9 August 2002
Online at stacks.iop.org/JPhysCM/14/R859

Abstract

The addition of non-adsorbing polymer to a colloidal suspension induces an interparticle 'depletion' attraction whose range and depth can be 'tuned' independently by altering the polymer's molecular weight and concentration respectively. Over the past decade, one particularly simple experimental realization of such a mixture has been studied in considerable detail: nearly-hard-sphere particles of poly(methyl methacrylate) and random-coil polystyrene dispersed in simple hydrocarbon solvents (mainly *cis*-decalin). The simplicity of the system has enabled rather detailed comparison of experimental findings with theory and simulation. Here I review the current understanding of the equilibrium phase behaviour, structure, phase transition kinetics, and metastability of this model colloid–polymer mixture. These findings form a useful reference point for understanding more complex mixtures. Moreover, in some cases, insights gained from studying this model system have relevance beyond soft-condensed-matter physics, e.g. in understanding the liquid state, in controlling protein crystallization, and in elucidating the nature of glasses.

(Some figures in this article are in colour only in the electronic version)

Contents

1. Introduction

The work of Peter Pusey with his collaborators in the 1980s established that suspensions of poly(methyl methacrylate) (PMMA) particles sterically stabilized by chemically grafted poly-12-hydroxystearic acid (PHSA) behaved like almost perfect hard spheres. Their equilibrium phase behaviour in the test tube matched that predicted by computer simulations, showing coexistence of colloidal fluid and crystal phases in the range $0.494 < \phi < 0.545$ (where ϕ is the volume fraction) [1]. The colloidal crystals were found, using static light scattering, to consist of hexagonally packed layers of particles stacked in a random sequence [2], consistent with the simulation result that face-centred cubic and hexagonal close-packed arrangements of hard spheres would have very similar free energies [3] (more accurate simulations have since been achieved using novel methods; see, e.g., [4]). The diffusive dynamics of the particles within the fluid phase, probed by dynamic light scattering, were also consistent with them being hard spheres [5]. A glass transition occurred at $\phi_g \sim 0.58$, where the 'caging' of particles by their neighbours became essentially permanent and rearrangements leading to crystallization did not occur [1]. The non-decaying component of the density fluctuations in the glass phase, again probed by dynamic light scattering [6], showed significant agreement with some of the first calculations made on hard-sphere glasses using mode-coupling theory [7]. Finally, binary mixtures of PMMA particles with specific ratio of radii were found to give rise to various superlattice, or alloy, phases at high densities [8], consistent with simulations based on packing considerations [9].

Many of these achievements were ably reviewed by Peter himself in his Les Houches notes [10], published in the same year that he took up the Chair of Physics in Edinburgh. In these notes, Peter described the 'colloids as atoms' approach. Since colloids undergo Brownian motion, they explore configurational space and will, given time, come to thermodynamic equilibrium. The tools of statistical mechanics, honed in the context of atomic and molecular materials, can therefore be 'borrowed' to discuss the behaviour of colloids. This approach is likely to be particularly fruitful in cases where the particles have well-characterized size, shape, and interaction—'model colloids'. Peter's own work on hard-sphere PMMA particles has done much to establish this 'paradigm' for modern colloid physics. (For a historical perspective on this approach, see the article by Haw in this Special Issue [11].)

When, as a complete novice to colloids, I read Peter's Les Houches review in 1991, the brief section on colloid–polymer (CP) mixtures particularly held my attention. The exclusion of polymer from the region between two nearby particles leads to an unbalanced osmotic pressure pushing them together [12, 13], which can be modelled as an 'effective attraction'; figure 1. The range and depth of this 'depletion attraction' are controlled by the polymer's size and concentration respectively. The simplest conceivable system of this kind (at least for a physicist!) would be hard spheres mixed with a non-adsorbing polymer, where the latter is itself dissolved in a 'theta solvent' with the result that their mutual interaction is minimal (i.e. the polymers are close to being 'ideal'). In an important paper, Gast *et al* had already calculated the phase behaviour of just such a mixture [14], but the full range of their predictions had not been unequivocally confirmed in the early 1990s (e.g. there was no report of three-phase coexistence); the experimental literature in fact contained a number of observations that did not fit within the theoretical scheme (e.g. some of the optical micrographs published by Sperry suggested various non-equilibrium aggregates [15]).

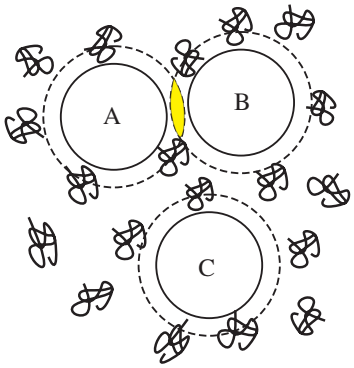

Figure 1. A schematic illustration of the depletion interaction. The centre of a polymer molecule (coil) is excluded from coming closer than a certain distance, approximately its own radius of gyration, to the surface of a colloid (full circle) because of the high entropic cost of configurational distortion. Each colloid is therefore surrounded by a depletion zone (dotted circle) within which there is essentially no polymer centres of mass. If a colloid (such as C) is far away from other particles, the osmotic pressure of the polymer on the particle is isotropic. If, however, the surface of two colloids (such as A and B) are closer than twice the size of a depletion zone, then there is no polymer in the lens-shaped (shaded) region, and a net (osmotic) force presses the particles together—the depletion attraction.

Reading Peter's Les Houches review and in discussions with him, it seemed to me in 1991 that the basic physics of CP mixtures should be a fruitful field for investigation (see also the historical remarks by Piazza in this Special Issue [16]). Moreover, Peter's work had rendered PMMA particles a good model system for just such investigations, provided that a suitable well-characterized, non-adsorbing, close-to-ideal polymer could be found. Polystyrene (PS) dissolved in the hydrocarbon solvents typically used for dispersing PMMA colloids (particularly *cis*-decalin) turned out to be just such a polymer. Much of the work of the Edinburgh group over the last decade has been devoted to the exploration of the effect of adding PS to PMMA suspensions, both as a basis to understand more complex mixtures, and as a laboratory for elucidating generic issues in condensed matter and statistical physics. More recently, other groups have also contributed new data on this system. To date, it is perhaps the most comprehensively explored CP mixture in the literature. Information on this model system has so far not been brought together in one place. A Special Issue in honour of Peter's 60th birthday seems a good place to do this. Below, I briefly describe our model CP system, and then successively review what is known about its equilibrium phase behaviour and structure, phase transition kinetics, and long-lived metastable states (glasses and gels), identifying gaps in our knowledge as I go along.

I should stress that the experimental, theoretical, and simulational literature on CP mixtures is large and growing. What follows is *not* intended in any way as a review of this literature. (Indeed, such a comprehensive review remains to be written.) My aim is far more limited—to summarize and discuss what is known about a particularly well-studied, very simple experimental model system. I take this opportunity to discuss some issues arising out of earlier publications that have become clearer with subsequent investigations, and to present a number of somewhat heuristic explanations for various observations. A very brief review of some of the same material has been given before [17].

2. The system

Sterically-stabilized PMMA particles were synthesized according to published procedures [18]. Some of the evidence that they behave as almost perfect hard spheres have already been briefly reviewed in the previous section (see also [19]). In our experiments, they were dispersed mainly in *cis*-decahydronaphthalene (*cis*-decalin). Sometimes, in order to match the refractive index of the particles to that of the dispersing medium, tetrahydronaphthalene (tetralin) was added. Tetralin is absorbed to a certain extent by the particles, giving rise to swelling over the course of days to weeks [20]. Particle radii were measured by static and/or

dynamic light scattering. The volume fractions of colloid stock solutions were determined by bringing them into the crystal–fluid coexistence region and measuring the fraction of the total volume occupied by the crystalline phase.

The interaction between PHSA brushes grafted onto PMMA under conditions closely similar to those on the surface of our model colloids has been measured directly using atomic force microscopy [21]. As expected, the potential rises to many k_BT over a few nm after the PHSA brushes touch each other. This small degree of softness makes no difference to the physics surveyed in this review. (However, the contribution by Auer and Frenkel in this Special Issue shows that a small degree of softness very significantly changes crystal nucleation rates [22].)

The polymer we used was random-coil PS. Its properties in a range of hydrocarbon solvents have long ago been characterized in detail by Berry [23]. In particular, Berry found that *cis*-decalin was a theta solvent for PS with $T_\theta = 286$ K. The extent to which it becomes non-ideal away from T_θ is measured by the dimensionless 'Fixman parameter', z, which depends the temperature T and the polymer molecular weight M_w according to

$$z = 0.009\,75\sqrt{M_w\ (\text{daltons})}\left(1 - \frac{T_\theta}{T}\right). \tag{1}$$

The radius of gyration at T_θ was found to scale (as expected) with the square root of M_w:

$$r_g^{(\theta)}\ (\text{nm}) = 0.028\sqrt{M_w\ (\text{daltons})}. \tag{2}$$

Away from T_θ, Berry determined the coil swelling, $r_g/r_g^{(\theta)}$, as a function of z. Our experiments were typically performed at a temperature of 292 ± 2 K, where coils should be slightly swollen. The radii of gyration of the PS used in our experiments were typically estimated using Berry's results, although direct checks using dynamic light scattering were made from time to time (see, e.g., [24]).

The interaction between PMMA particles and PS has not been measured directly to date. It is *a priori* plausible they should be mutually non-adsorbing. The chemically grafted PHSA layer on the PMMA particles functions as steric stabilization because it is in a good solvent; *cis*-decalin is a better-than-theta solvent for PS at room temperature. We therefore expect mutual repulsion. Diffusion measurements of very dilute PMMA particles in a *cis*-decalin solution of PS returned values of the hydrodynamic radius that were consistent with no adsorption [20].

Using laser trapping of particles ('optical tweezers'), it is now possible to measure directly forces (see, e.g., [25]) and therefore interaction potentials in the colloidal domain. The depletion attraction induced by non-adsorbing polymers between a particle and a hard wall (essentially another particle with infinite radius) has been measured directly in this way (e.g. [26]). It would be of interest to carry out such measurement in our system, which, amongst other things, should provide more evidence for non-adsorption. Very interestingly, Starrs and Bartlett have recently measured the correlated fluctuations of two PMMA particles in a solution of PS in *trans*-decalin using optical tweezers [27]; their data are consistent with the presence of a depletion zone of polymers round each particle.

3. Equilibrium phase behaviour

3.1. Hard spheres and near-ideal polymer: how to make a liquid

The equilibrium phase diagrams of PMMA particles with $R \sim 220$ nm mixed with PS of three different molecular weights are shown in figure 2 [28]. The theory of Gast *et al* [14] predicts that the topology of the phase diagram depends on the range of the depletion attraction, which as a

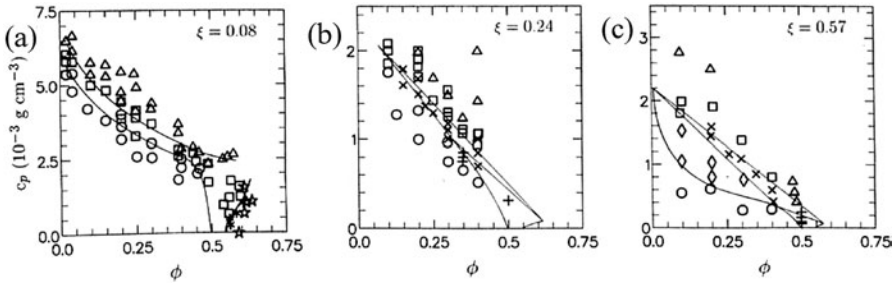

Figure 2. The phase diagram of PMMA colloids and PS polymer dispersed in *cis*-decalin at 292 K at three size ratios (ξ, given in figures). Horizontal axis: colloid volume fraction (ϕ); vertical axis: polymer concentration (c_p). Circles = fluid, diamonds = gas + liquid, crosses = gas + liquid + crystal, plus signs = liquid + crystal, squares = gas + crystal, triangles = aggregation/gel, stars = glass. Curves are guides to the eye to the boundaries of the various multiphasic regions. Reproduced from [28].

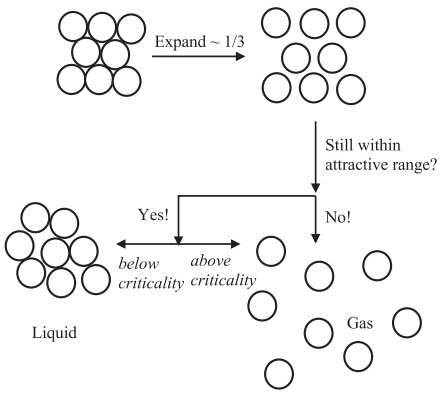

Figure 3. A schematic illustration of why an interparticle attraction of long enough range is needed for a thermodynamically stable liquid phase to occur.

fraction of the hard-sphere diameter can be estimated by $\xi = r_g/R$. As predicted, the addition of sufficiently small polymers ($\xi \sim 0.08$) merely expands the fluid–crystal coexistence region of the parent hard-sphere system. In accordance with the 'primitive model' of Lekkerkerker *et al* [29], the tie lines in the fluid–crystal coexistence region were found to be slanted [24], indicating polymer partitioning between the coexisting phases. At larger ξ, a critical point appears in the phase diagram. Referring to the phase diagram for $\xi \sim 0.57$, we found that at moderate volume fractions (say, $\phi \sim 0.2$), progressive addition of polymer brought about gas–liquid coexistence, gas–liquid–crystal coexistence, and gas–crystal coexistence. Note that triple coexistence can be observed in an extended, triangular region in the phase diagram. At a crossover value of $\xi_c \sim 0.24$, a liquid phase still exists, as indicated by the observation of a finite triple-coexistence region; but the width of the gas–liquid region has become unobservably narrow.

These experimental results confirm that an interparticle attraction (here a depletion attraction) of sufficiently long range is needed for a thermodynamically stable liquid phase to exist. This can be understood heuristically by the following argument, summarized schematically in figure 3. (This argument was suggested to me in outline by Peter Pusey some years ago, and first sketched out in [30].)

In a system of (classical) particles with long-range attraction, the melting transition is (like in hard spheres) entropically driven (since the potential experienced by each particle due to the

sum of contributions from its neighbours should be essentially flat, giving a trivial, constant internal energy contribution to the free energy [31]). When the close-packed crystal ($\phi \approx 0.74$ in hard spheres) expands in volume by about one third (to $\phi = 0.545$ in hard spheres), rigidity is lost. (This is the physics behind the 'Lindemann criterion' for melting [32].) Now consider the effect of shrinking the range of the interparticle attraction.

If, at the point of loss of rigidity, neighbours are still within range of each others' attractive potential, a dense liquid phase is possible—whether it actually occurs then depends on whether the thermal energy is enough to enable particles to overcome their mutual attraction (i.e. whether one is above or below the critical point). If, however, the range of the interparticle attraction is shorter than a certain critical value, expansion of the crystal to the point of loss of rigidity would bring neighbours out of range of each other's attraction, so the crystal would catastrophically fall apart, giving a low-density gas. Expansion of the density by $\sim 1/3$ corresponds to a $\sim 10\%$ increase in the average interparticle spacing (cf the Lindemann criterion). If the interparticle attraction has a range of about twice this, then in the crystal at melting density, each particle will always stay within range of its neighbours as it executes thermal motion in the cage formed by these neighbours. This argument therefore suggests a crossover when the range of interparticle attraction is ~ 0.2 of the hard-core repulsion.

This line of reasoning should apply directly to particles that have a simple attraction for one another. So it is interesting that simulations of hard particles with a Yukawa tail predict that the gas–liquid critical point disappears when the Yukawa range is less than about one sixth (~ 0.16) that of the hard-core diameter [33]. An effective two-body depletion attraction only captures part of the physics in a CP mixture. Thus the experimental value of $\xi_c \sim 0.24$ in our model system only provides partial support for the scheme suggested above. Note that simple theories for CP mixtures return a value of $\xi_c \sim 0.3$ [14, 29] (see further: section 3.4 below).

The fluid–crystal coexistence boundary in our simple model system at $\xi < \xi_c$ can be mapped onto that of globular protein solutions if the strength of the interparticle attraction is measured in terms of the second virial coefficient [34]. This suggests that at least for some purposes, complex globular proteins can be approximated simply as 'sticky particles'.

3.2. Effect of temperature, polymer non-ideality, and polydispersity on phase behaviour

3.2.1. Temperature and polymer non-ideality. Increasing the temperature of our model CP mixture has at least two qualitatively distinct effects on its equilibrium phase behaviour. First, because the polymer coils expand, the size ratio ξ changes. This effect is what the simple theories of Gast *et al* [14] and Lekkerkerker *et al* [29] addressed. However, changing the temperature also changes the degree of coil non-ideality (see equation (1)).

A simple perturbative treatment taking into account changing size ratios and polymer non-ideality [35] found that at temperatures just above T_θ there was no systematic movement of the phase boundaries (i.e. they do not all move up or all move down in the phase diagram). This is consistent with the limited data available at that time for both $\xi < \xi_c$ [24] and $\xi > \xi_c$ [35]. Recent, more detailed experiments support this general conclusion, although a number of interesting details have been found [36].

An attempt to isolate the effect of polymer non-ideality can be made by changing the polymer topology and keeping $\xi = r_g/R$ constant. This can be done using star polymers. A star polymer of functionality f consists of f linear chains bonded to a common centre. (In particular, a star with $f = 2$ is a linear chain.) It is known that as f increases, the polymer–polymer (PP) interaction becomes increasingly non-ideal, approaching that between hard spheres at very large f [37]; the polymer–colloid interaction also becomes increasingly hard [38].

We recently investigated the phase behaviour of a colloid + star polymer mixture in which star polymers of various f but (approximately) constant r_g were mixed with PMMA colloids [39]. The arms in the star were made of polybutadiene, for which *cis*-decalin is a good solvent. (Thus the $f = 2$ data were not directly comparable to the 'standard model' of PMMA particles and PS in *cis*-decalin, where the polymer is almost ideal.) The size ratio $\xi = r_g/R$ was kept constant at ∼0.5. We found that the phase diagram for the $f = 2$, 6, 16, and 32 mixtures were topologically identical to that shown in figure 2(c). However, the stability of the liquid phase progressively decreased with increasing f. (Observationally, the size of the gas–liquid coexistence region shrinks.) Extrapolating from these findings, we speculated that a mixture of $f = 64$ star polymers and hard-sphere colloids at this size ratio might behave as a binary hard-sphere mixture as far as phase behaviour was concerned. Thus we may expect superlattice structures of the AB_2 and AB_{13} kind first discovered by Peter and his co-workers [8, 9] using two-sized mixtures of PMMA particles. The synthetic opportunities offered by star polymers opens up the possibility of self-assembling binary colloidal crystals with two species that have very different functional characteristics.

3.2.2. Polydispersity. Real colloids are necessarily polydisperse. This fact is often regarded as an inconvenience in the study of phase transitions by colloid physicists, the assumption being that polydispersity has little that is of fundamental importance to reveal. The overwhelming majority of theories/simulations simply ignore it altogether. One exception was a short paper by Peter Pusey [40] in which he suggested that the maximum polydispersity for hard-sphere crystallization could be estimated by

$$\sigma_{\max} = \left(\frac{\phi_{cp}}{\phi_m}\right)^{1/3} - 1, \tag{3}$$

where $\phi_{cp} = \pi/\sqrt{18} \approx 0.74$ is the maximum (close-packing) volume fraction of crystals and $\phi_m = 0.545$ is the hard-sphere melting volume fraction. The physical content of this estimate is simply that the whole distribution of particle sizes could be accommodated, just, by the 'rattling room' available to the crystal at melting (cf the Lindemann criterion for melting). Equation (3) gives $\sigma_{\max} \approx 11\%$, in almost perfect agreement with experimental observations.

This 'Pusey–Lindemann' argument can be turned on its head to make an interesting prediction on the effect of polydispersity for CP mixtures [41]. At small ξ, adding polymer merely expands the fluid–crystal coexistence region in the phase diagram (cf figure 2(a)). This means that at progressively highly polymer concentrations, increasingly dense crystals, with $\phi \to \phi_{cp}$, coexist with increasingly dilute gas, with $\phi \to 0$. The Pusey–Lindemann argument then suggests that for a given polydispersity $\sigma < 11\%$, crystallization should become impossible beyond a certain critical polymer concentration; the density of crystals at this polymer concentration is related to σ by equation (3). This has been confirmed by experiments [41, 42].

Polydispersity is, in fact, an interesting phenomenon in its own right. How to calculate the equilibrium phase behaviour of an effectively infinite-component system, in particular how to obtain the particle size distributions in coexisting phases ('fractionation'), is a problem that has attracted considerable attention recently (see the review in [43]). We have studied phase separation in PMMA colloid with $\sigma = 0.18$—too polydisperse to give colloidal crystals [40]—with added PS at the (average) size ratio $\langle\xi\rangle \sim 0.54$ [41, 44]. The only multiphasic region in the phase diagram of this system is that of gas–liquid coexistence (cf removing the crystal phase from the phase diagram in figure 2(c)). Experiments showed that the phase separation produced significant fractionation of the colloid, with the bigger particles being found in the denser, liquid phase. This is intuitively reasonable, since the depletion attraction is greater for

larger particles [12, 13]. Detailed measurements revealed that, within experimental error, the first three moments of the particle size distributions in the coexisting gas and liquid phases obey the following relationship:

$$\frac{\Delta R}{\langle R \rangle} = \left(\frac{\sigma_P^2}{\tau_P^3} \right) \Delta\sigma^2. \tag{4}$$

Here ΔR and $\Delta\sigma^2$ are the difference in average radii and squared polydispersity between coexisting phases, and $\langle R \rangle$, σ_P^2, and τ_P^3 are first, second, and third moments of the particle size distribution of the parent colloid before phase separation (defined with suitable normalization—see [44, 45] for details). The conditions under which this and other 'moment relations' may hold in polydisperse phase separation has been analysed [46].

The effect of polydispersity on the phase behaviour of a hard-sphere + polydisperse ideal linear polymer mixture has also been analysed theoretically [47, 48] using a generalization of the approach of Lekkerkerker *et al* [29] but has not, to our knowledge, been studied experimentally. Very recently, however, we have studied phase separation in a mixture of PS spheres and worm-like surfactant micelles [49]. These micelles behave as a solution of highly polydisperse (living) polymers. The position of the gas–liquid phase boundary is reasonably well predicted [50] by incorporating the living-polymer size polydispersity into the free volume approach [29].

3.3. Equilibrium structure and particle dynamics

Compared to the relatively detailed investigation of equilibrium phase behaviour already reviewed, there is little information on the equilibrium structure of the various phases in our model CP mixture. Even less is known about the dynamics of such systems at thermal equilibrium.

The only detailed investigation of equilibrium structure [30] was performed on a sequence of three colloidal liquids at triple coexistence (i.e. the liquid corner of the three-phase triangle; see figure 2(b) or (c)) with progressively smaller ξ. As the crossover polymer-to-colloid size ratio, ξ_c, is approached, the gas–liquid critical point merges with the gas–liquid edge of the triple triangle (cf figures 2(c) and (b)). The liquid state at triple coexistence at or around ξ_c should therefore show critical features, e.g. long-range density fluctuations. Such fluctuations were indeed found by measurement of the colloid–colloid (CC) static structure factor, $S_{CC}(Q)$ (where Q is the magnitude of the scattering vector) using a novel application of 'two-colour dynamic light scattering' [51]. $S_{CC}(0)$ provides a measure of the amplitude of fluctuations in the colloid density; figure 4 suggests that its value is highest for the system with $\xi = 0.24$, which is very close to the crossover size ratio in our system (see figure 2(c)). This trend of increasing fluctuations as one approaches ξ_c was also seen by direct observation using phase contrast microscopy.

No measurement of the structure of colloidal crystals in our model CP mixture has been attempted to date; in particular. In the case when ξ is small, the short-range nature of the effective interparticle attraction suggests that the free energy difference between different stacking sequences of hexagonal planes will again be small, so we expect random stacking.

3.4. Comparison with theory

There has been much recent theoretical and simulational effort in calculating the equilibrium phase behaviour of simple CP mixtures and the structure of non-ordered (fluid) states. The following table summarizes a number of different approaches. When both gas–liquid binodals

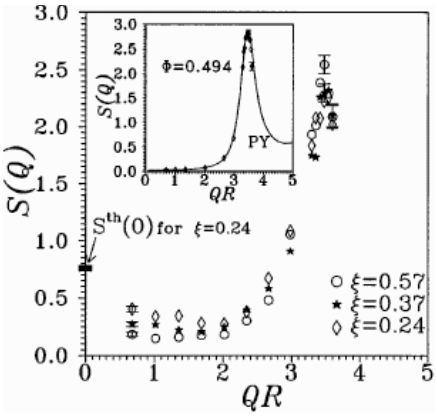

Figure 4. Measured static CC structure factors, $S_{CC}(Q)$, of the colloidal liquid at triple coexistence of a model CP mixture at size ratios $\xi = 0.58$, 0.37, and 0.24 (key inside figure); Q is the magnitude of the scattering vector, and R the colloid radius. Note the rise in the low-Q amplitude as ξ is decreased towards the experimental crossover size ratio of 0.24. The calculated value of $S(0)$ for the crossover size ratio according to the theory in [29] is indicated by a bold tick on the vertical axis. These measurements were performed using a novel application of two-colour dynamic light scattering [51]; the inset shows the $S(Q)$ for pure hard spheres measured using this method at $\phi = 0.494$ (points) compared to the theoretical (Percus–Yevick) result (curve). Reproduced from [30].

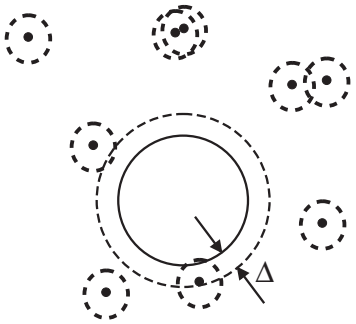

Figure 5. A schematic diagram of the AO model for a CP mixture. Colloids are hard spheres. Polymers are points and do not interact with each other (so they can overlap). However, the points are excluded from coming closer than a distance Δ from the surface of a colloid, where Δ is close to (and certainly supposed to scale as) the real polymer's radius of gyration.

Table 1. Theory and simulation of model CP mixtures.

Model	Polymer	Gas–liquid	Crystal	ξ_c	$S(Q)$
PTAO [14]	Non-additive points	Y	Y	0.32	N
MFAO [29]	Non-additive points	Y	Y	0.32	N
LP [52]	Ideal random walk	Y	Y	0.45	N
PYAO [53]	Non-additive points	N	N	—	Y
EPAO [54]	Non-additive points	Y	Y	$\gtrsim$0.4	Y
SIMAO [55]	Non-additive points	Y	N	—	N
EPIP [55]	Self-avoiding walk	Y	Y	0.34	Y
PRISM [56]	Interacting ideal coils	Y [57]	N	—	Y
ST [58]	ST	Y	Y	—	N

('gas–liquid' in the table) and the melting/freezing lines ('crystal' in the table) are calculated, the size ratio above which a critical point appears in the phase diagram, ξ_c, can be determined. Some authors also calculate static (CC) structure factors, $S(Q)$. The different methods differ chiefly in the way the polymer is treated, and then in the methods used to solve the statistical mechanics. (I have tried to capture these two aspects in the acronyms given: see the explanation in the following discussion.)

The pioneering work of Gast *et al* [14] used thermodynamic perturbation theory (PT) to calculate the phase behaviour of hard spheres with an added depletion potential of Asakura–Oosawa (AO) form [13]. Subsequently Lekkerkerker *et al* [29] calculated the mean-field (MF) phase diagrams of the AO model. In this model, figure 5, colloids are hard spheres; polymers are points that do not interact with each other, but are excluded from coming closer than a

certain distance from the colloidal surface (usually identified as something like the polymer's radius of gyration).

Subsequently Meijer and Frenkel [52] simulated spheres mixed with ideal lattice polymers (LP) and obtained full phase diagrams. Louis *et al* [53] solved for structure factors of the AO model using Percus–Yevick closure (PYAO). Later, the same group also obtained the gas–liquid coexistence curves of the AO model from simulations (SIMAO) as well as calculated full phase diagrams by obtaining effective potentials between colloids and interacting polymers (EPIP) [55]. Dijkstra *et al* obtained the effective potential between colloids in the AO model (EPAO) using simulations and then calculated full phase diagrams as well as structure factors [54]. Fuchs *et al* [56, 57] sought to take account of internal degrees of freedom of the polymer using an extended version of the 'interaction site model' from liquid-state theory (PRISM). Finally, in their contribution to this Special Issue, Lekkerkerker and co-workers used results from polymer scaling theory (ST) to calculate full phase diagrams [58] within the framework of the earlier free volume approach [29].

It is not the purpose of this review to discuss these theories and simulations in detail. Nevertheless, certain features emerging from this ongoing effort are worth bringing out. First, it is clear that the gross feature of 'no liquid state unless the polymer is large enough' is robust. Secondly, as expected, the larger the size ratio, the more distinct the different models become. The third feature to emerge from recent theory/simulation is that quantitative aspects, in particular the positions of various boundaries in the phase diagram and static structure factors, are very sensitive to the detailed assumptions and approximations used in various calculations. This means that quantitative comparison between theory, simulation, and experiment should proceed with care.

Simulations (SIMAO [55]) show that simple approximate schemes [14, 29] give rather accurate predictions to the gas–liquid binodal of the AO model at large size ratios ($\xi \sim 1$). These simple approximate schemes are not so accurate *as solutions to the AO model* at smaller ξ. However, it turns out that they give tolerably good accounts of the overall positions of the phase boundaries of our CP mixture as size ratios $\xi \sim 0.08$ and 0.57 (see the comparisons in [28]). Two caveats should, however, accompany this statement. First, these simple theories predict too high a value ($\gtrsim$0.3) for the crossover size ratio above which a gas–liquid critical point appears in the phase diagram (see figure 2). The experimental phase diagram at $\xi^{\rm expt} \sim 0.57$ is relatively further away from the experimental crossover at $\xi_{\rm c}^{\rm expt} \sim 0.24$ than the theoretical phase diagram at $\xi^{\rm th} = 0.57$ is from the theoretical crossover predicted at $\xi_{\rm c}^{\rm th} \sim 0.3$. Arguably, the experiment and theory should be compared at the same value of $(\xi - \xi_{\rm c})/\xi_{\rm c}$, so the experimental phase diagram at $\xi \sim 0.57$ ought to be compared with the theoretical one at $\xi \sim 0.76$. The same point can be made in comparing other measurements (such that those of structure) with predictions. Note that it is a 'robust' feature of all theories and simulations to date that they give values of $\xi_{\rm c}$ significantly larger than those obtained from experiments (ours, as well as data from a more complex system [59]). This puzzling disagreement remains to be resolved.

The second caveat is that the simple theories of [14, 29] underestimate by a few orders of magnitude the amount of polymer present in the triply-coexisting liquid phase in phase diagrams with $\xi > \xi_{\rm c}$ (see the estimated positions of the phase boundaries in figure 2(c), as well as explicit measurements for the case of $\xi \sim 0.37$ in [30, 60]). Equivalently, these approximate solutions to the AO model predict far too small a region of liquid–crystal coexistence. Theories that take more realistic account of the polymer are significantly more successful in this respect: the polymer concentrations of the triple-coexistence liquids in [55] and [58] agree with experiments to much better than order of magnitude. (Gas–liquid spinodals have been calculated using PRISM theory [56]; from these one could estimate an order of

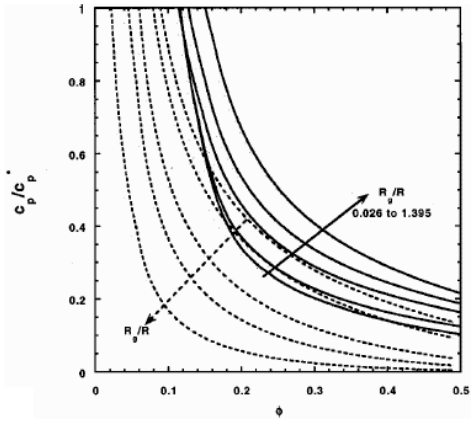

Figure 6. Movement of the gas–liquid spinodal as ξ increases from 0.026 to 1.395 (in the direction of the arrows) according to PRISM (full curves) and MFAO (dotted curves). Horizontal axis: colloid volume fraction (ϕ); vertical axis: polymer concentration in units of the overlap concentration (c_p/c_p^*). Reproduced with permission from [57].

magnitude for the polymer concentration for the triple-coexistence liquid, which also agrees much better with experiments.) One reason for the presence of much more polymer than simple theories would lead us to expect is that the depletion zone thickness decreases with increasing polymer concentration [58], a feature that can only emerge when there is some realism in treating the polymers.

Turning to the movement of phase boundaries, the prediction of the PRISM model [56] directly contradicts that of the PTAO/MFAO models [14, 29], figure 6. Experiments using another model system in the group of Zukoski confirmed the PRISM model, that is to say, the gas–liquid boundary moves up in the phase diagram if polymer concentration is given in units of the overlap concentration [57]. Note, that in the Zukoski model system, the polymers are in a good (athermal) solvent, while the PRISM model has been solved for a somewhat artificial 'hybrid': interacting Gaussian coils. Corresponding experiments in the PMMA colloids + PS systems remain to be performed.

Finally, there have been few comparisons with experiments in terms of structure. In our model system, the only published data are CC structure factors, $S_{CC}(Q)$, of the colloidal liquids at triple coexistence at three values of ξ [30]. Available comparisons of these with theory/simulation [53, 54, 56] show reasonable agreement in terms of the rising amplitudes at low Q as $\xi \to \xi_c$ and an invariant main peak position. Experimentally, however, it was found that the main peak height also remained more or less constant as ξ changes; this aspect has not so far been reproduced by theory/simulation.

Note that a full characterization of the structure of a CP mixture requires, in principle, knowledge of the correlation between colloids, between monomers on the polymer and other monomers (same or different chain), as well as between monomers and colloids. Even with the drastic simplification of considering only the centre of mass of each polymer (thus ignoring potential distortion of the average polymer shape [52]), three partial structure factors are required, CC, CP, and PP. There are some data for $S_{CC}(Q)$ [30]. I am not aware of published measurements of any other structure factors for our model system or of any other CP mixtures. Careful contrast matching using partially deuterated colloids, polymers, and solvent can, in principle, give significant progress here. A note of caution, however, is in order. Using deuterated polymers and/or solvent will undoubtedly cause movements in the phase boundary due to changes in the polymer size and non-ideality; it may therefore be difficult to ensure that different samples in a contrast-variation series in fact correspond to closely similar thermodynamic state points.

4. Phase transition kinetics

In principle, information on phase transition kinetics and metastability comes free during experimental determination of the equilibrium phase behaviour. In a typical experiment of the latter kind, a sample of the correct overall composition (colloid and polymer concentrations) is made up in a cuvette and tumbled to ensure homogenization. Then the homogenized sample is left undisturbed for observation. If its composition is in a multiphasic region of the phase diagram, phase separation should occur in the course of time. If the particles are not density matched to the solvent, then phase separation will lead to the appearance of macroscopic regions of different compositions. These regions can often be visually distinguished by their different scattering properties (most obviously, colloidal crystallites are iridescent). What I have just described is a *process* that takes anything from hours to days to complete in our model CP mixture. Rather detailed information on phase transition kinetics can therefore be obtained using a variety of methods—from observation by the naked eye through various imaging techniques to light scattering. Moreover, the kinetic process can get stuck in long-lived metastable states; this is a hindrance as far as studying equilibrium phase behaviour is concerned; but the study of metastability is a burgeoning field of condensed matter and statistical physics in its own right. In this and the next section, I review what is known about the phase transition kinetics and metastability of mixtures of PMMA colloids and random-coil PS polymers. (For a brief overview of kinetics and metastability studies on pure PMMA colloids, see [61].)

Perhaps the simplest study of phase transition kinetics one could imagine in a model CP mixture is the homogeneous nucleation of colloidal crystal in a system with $\xi < \xi_c$, with the sort of phase diagram shown in figure 2(a). The addition of polymer in this case simply widens the crystal–fluid coexistence region of pure hard spheres. There is significant knowledge of crystal nucleation in pure PMMA colloids from light scattering [62] and microscopy [63, 64]. Simulations of the nucleation rate are also available for direct comparison with experimental data [65]. The kinetics of homogeneous nucleation of colloidal crystals in the expanded fluid–crystal coexistence region in CP mixtures at low ξ has not been studied. Building on recently emerging results on hard-sphere [65] and soft-sphere nucleation [22], it would certainly be of interest to know how a short-range interparticle attraction affects nucleation kinetics. It would also be of interest to know whether the effective potential picture is adequate for modelling kinetics, or whether, for this purpose, it is essential to treat the colloid and polymer on an equal footing and consider binary nucleation (see, e.g., the discussion and references in [66]).

While single-stepped, homogeneous nucleation has not been studied in the small-ξ regime of our model CP mixture, this system has been used to study perhaps one of the simplest examples of a multi-stepped kinetic pathway. To see why this is the case, consider what happens to the gas–liquid binodal when ξ becomes progressively smaller. When it 'disappears' from the equilibrium phase diagram at $\xi < \xi_c$, it can be considered as having gone into 'hiding' as a 'metastable phase boundary' in the equilibrium fluid–crystal coexistence region, figure 7(a). A more formal version of this statement can be made by considering the free energy of our system. Just inside the fluid–crystal coexistence region, only a single 'common tangent' can be constructed between the fluid and crystal branches, the cotangency points giving the densities of coexisting fluid and crystal phases, figure 7(b). At higher polymer concentrations, however, the fluid branch develops a point of inflection, figure 7(c); thereafter, a common tangent can be constructed on this branch alone, giving the densities of two coexisting fluid phases (gas and liquid), which can be plotted as a gas–liquid binodal completely buried within the equilibrium fluid–crystal coexistence region.

This fluid–fluid coexistence is metastable relative to the fluid–crystal coexistence given by the common tangent between the fluid and crystal branches. Thus, in the long run (i.e. when

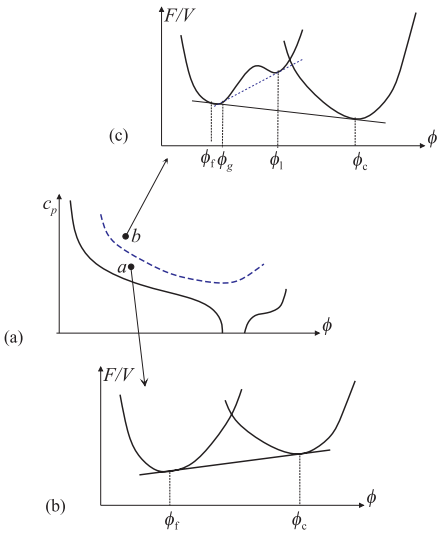

Figure 7. (a) A schematic diagram of the metastable gas–liquid binodal 'buried' within the equilibrium fluid–crystal coexistence region in the phase diagram of a CP mixture at low ξ (say, ∼0.1; cf figure 2(a)). Above the bold curve and below the dashed curve, homogeneous nucleation of colloidal crystals should occur. Above the dashed curve, the system can also undergo (metastable) gas–liquid phase separation *en route* to crystallization. (b) The free energy density (F/V) of a sample at point 'a'. A single double tangent can be constructed between the fluid and crystal branches, giving the densities of coexisting fluid (ϕ_f) and crystal (ϕ_c) phases. (c) The free energy density of a sample at point 'b'. The fluid branch now has double minima. The double tangent between these two minima gives the densities ϕ_g and ϕ_l on the metastable gas–liquid binodal (dashed curve in (a)). The double tangent between the fluid and crystal branch still gives the densities of the (thermodynamically stable) coexisting fluid and crystal phases (ϕ_f and ϕ_c).

equilibrium has been reached), one expects fluid–crystal coexistence. However, kinetically, one may expect gas–liquid phase separation to proceed faster than crystallization: it does not involve symmetry breaking, and (under the right conditions) it can proceed via the very fast route of spinodal decomposition. These considerations suggest that a homogeneous sample within the metastable gas–liquid binodal may first undergo gas–liquid phase separation, and only subsequently nucleate crystals to reach final equilibrium. Furthermore, we may expect the majority of crystals eventually to nucleate out of the metastable liquid phase, since it is considerably closer in density to the crystals than the gas phase with which it is in (metastable) coexistence.

That there is such a 'buried' gas–liquid binodal in the expanded fluid–crystal coexistence region was suggested in one of the first publications on our model system [24], and there were indeed early hints of incipient gas–liquid phase separation deep enough inside this region [67]. Due to complications from gelation (for which see the next section), 'clean' observation of a mixture at low ξ first undergoing gas–liquid phase separation and then homogeneous nucleation of colloidal crystals to give final fluid–crystal coexistence has only just been achieved [36, 68], in a system with $\xi \sim 0.22$ at $\gtrsim$30 °C. Note that this process is an instance of the 'Ostwald step rule' [69], which suggests that phase transformation proceeds via all metastable intermediates in turn. A similar, two-stepped crystallization mechanism has also been observed by Hobbie in a binary hard-sphere system (where the smaller spheres cause a depletion attraction between the bigger ones) [70].

A theoretical basis can be provided for this two-stepped phase separation scenario by solving for the dynamics of the interfaces between a metastable phase sandwiched between the two thermodynamically stable phases in a biphasic region. A simple one-dimensional model [71–73] shows that the width of the metastable region will grow just inside a metastable phase boundary buried within an equilibrium two-phase region.

The argument leading to the prediction of fluid–crystal phase separation *via* the intermediate step of gas–liquid phase separation can be generalized, using a line of reasoning first suggested by Cahn in the context of metallurgy [74]. Cahn's argument provides a means of carving up the equilibrium phase diagram into a map of different kinetic regimes where distinct kinetic pathways are variously permitted or disallowed. The case of the fluid–crystal

coexistence region for the low-ξ system already considered is an example. Just across the fluid–crystal coexistence boundary, homogeneous nucleation of crystals is the only permitted kinetic pathway. Across the metastable gas–liquid binodal, however, the two-stepped mechanism sketched above becomes also possible; an educated guess suggests that this mechanism should dominate, at least initially. The same procedure has been applied in detail to homogeneous samples within the triple triangle in a system with $\xi \sim 0.37$ (cf the phase diagram topology in figure 2(c)) as they separate into coexisting gas, liquid, and crystal phases [60, 75]. A pedagogical discussion of how to turn equilibrium phase diagrams into such kinetic maps applicable to any soft-matter system can be found in [76].

A further interesting kinetic issue that could, in principle, be addressed using our model system is that of the influence of a nearby gas–liquid critical point on crystal nucleation, an issue that has arisen in the context of protein crystallization [77]. An obvious way to study this issue is to investigate crystal nucleation in the vicinity of the critical point of the buried gas–liquid binodal in a system with small ξ (cf the discussion at the beginning of this section), although in practice gelation and other non-equilibrium aggregation phenomena may render the metastable critical point inaccessible (see the next section). More intriguingly, there is also the possibility of studying the nucleation of crystals from a homogeneous sample within the triple triangle in our model system with $\xi \sim 0.24$. The phase diagram in figure 2(b) shows that the gas–liquid critical point has practically merged into the gas–liquid edge of the triple triangle, so crystal nucleation in a three-phase coexistence sample in fact takes place close to a gas–liquid critical point. Such experiments remains to be carried out.

5. Long-lived metastable states: gels and glasses

When an off-equilibrium system evolves towards equilibrium, it sometimes finds itself 'stuck' in long-lived metastable states with rather well-defined bulk properties that only very slowly change with time. Understanding such long-lived metastable states is one of the outstanding challenges facing 21st century physics; it is also very important for practical applications—many industrial products (and, in fact, all living systems!) are in long-lived metastable states. In this section, I review what is known about such states in our model CP mixture at small ξ; long-lived metastable states in systems with $\xi > \xi_c$ have been little studied to date.

5.1. The high-density limit: multiple glassy states

Equilibrium statistical mechanics predicts that the lowest free energy state for an assembly of hard spheres is fully crystalline at all volume fractions $\phi > 0.545$. Experimentally, non-density-matched PMMA colloids fail to crystallize above $\phi \sim 0.58$ [1]. The dynamic structure factor also fails to decay completely within rather long experimental time windows [6]. This has been interpreted as a glass transition occurring at $\phi_g \sim 0.58$ due to the caging of particles by their neighbours. Mode-coupling theory receives substantial support when applied to experimental data from PMMA colloidal glasses [78].

Using our model CP mixture with small ξ, we have recently studied how the hard-sphere glass transition is perturbed by a short-range interparticle attraction [79]. It turns out that the glass transition line is re-entrant; figure 8. Consider a sequence of samples at $\phi \sim 0.61$. The sample without polymer (A) is a pure hard-sphere glass. Addition of a little polymer 'melts' the glass, and brings about crystallization (e.g. sample B). The presence of even more polymer, however, leads to non-crystallization once more (e.g. samples C–E), suggesting another glass transition.

One possible (heuristic) explanation of this re-entrant glass transition is as follows; figure 9. In the pure hard-sphere glass, each particle is 'caged' by its neighbours. The presence of a

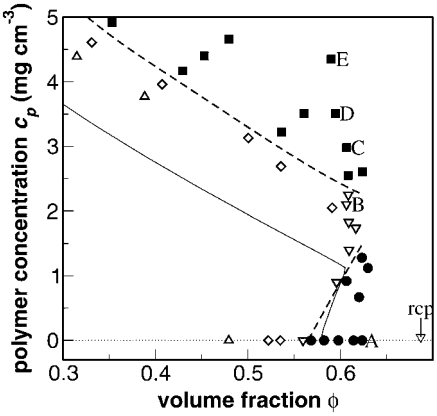

Figure 8. Equilibrium and non-equilibrium behaviour of a CP mixture at $\xi = 0.08$. Samples that reached thermal equilibrium (open symbols): fluid (triangles), fluid–crystal coexistence (diamonds), fully crystalline (inverted triangles); samples that did not reach thermal equilibrium (filled symbols): repulsion-driven glass (circles) and attraction-driven glasses (squares). Dashed curves: guides to the eye to the observed non-crystallization lines. Continuous curves: MCT predictions of glass transition lines. (rcp = estimated random close packing in this slightly polydisperse colloid.) Reproduced from [79].

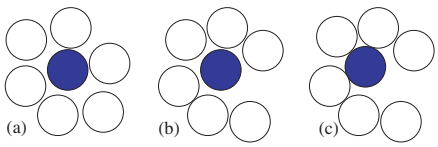

Figure 9. A schematic representation of the mechanism giving rise to the re-entrant glass transition shown in the previous figure. (a) A repulsion-dominated glass—the central (shaded) particle is caged by its neighbours (and also forms part of the cages of its neighbours). (b) A little short-range attraction leads to the clustering of the cage and opens up enough gap to allow the central particle to escape—the repulsion-dominated glass melts. (c) Sufficient short-range attraction, however, means the 'everything is stuck to everything else'—the system arrests again into an attraction-dominated glass. Note that this picture suggests a significantly higher degree of structural inhomogeneity in the attraction-dominated glass.

sufficiently deep short-range attraction, brought about by the addition of polymer, leads to clustering of the particles in the cage, so that long-range particle motion becomes possible again. The addition of even more polymer, however, leads to an interparticle attraction so deep that all particles are stuck to each other, once more giving rise to structural arrest. This leads us to distinguish between two types of glass—repulsion dominated, and attraction dominated. Dynamic light scattering provides support for this picture [79]: the non-decaying part of the dynamic structure factor in repulsion-dominated glasses is significantly smaller than that in attraction-dominated glasses. In the former, particles 'rattle' in their cages, while in the latter, they are confined by the (very short-range) interparticle attraction. Simulations and mode-coupling theory calculations also support this picture (see [79] and references therein).

Much remains to be done to elucidate the differences between these two kinds of glass. An obvious tool to employ to study them is confocal microscopy. (One synthesis of suitable fluorescent PMMA particles for confocal microscopy has been described recently [80].) Apart from the possibility of directly confirming the picture sketched in figure 9, confocal microscopy can also give information on, e.g., dynamic heterogeneities [81] (as has been done for pure hard-sphere colloidal glasses [82]). Mode-coupling theory predicts that the shear moduli of attraction-dominated glasses should be significantly higher than those for repulsion-dominated glasses [83]—this remains to be confirmed. We may also expect that the rotational diffusion of particles to be much more restricted in the attraction-dominated regime; this hypothesis can be tested using, for example, time-resolved phosphorescence depolarization [84]. One may expect that the ageing behaviour (essentially, dependence of the dynamics on the 'waiting time' between sample preparation and commencement of measurement) should be different for these two types of glass—detailed dynamic light scattering can throw light on this issue. Finally,

mode-coupling theory predicts that the re-entrant glass transition disappears when the interparticle attraction has long enough range [83]. This can be tested using our model system at high ξ.

It is tempting to speculate whether the existence of repulsion-and attraction-dominated glasses in such a simple model system may illuminate an issue that has been controversial in the atomic and molecular glass literature for some time (see, e.g., [85] and references therein): is the glass transition mainly temperature or volume/density driven? Stated differently, the issue is whether we have mainly an energetic or entropic effect. A recent study of triphenyl phosphite [85] found that around ambient pressure, energy (or temperature) is the dominant variable, although the authors suggested that at elevated pressure, density could become the dominant effect. In this language, our model system is driven to structural arrest in the repulsion-dominated regime by volume/density/entropy, while the attraction-dominated glass is arrested largely because of energy/density. There is thus at least a superficial resemblance. Whether there is any deeper connection remains to be seen.

5.2. Lower densities: clusters and gels

The existence of a metastable gas–liquid binodal buried in the equilibrium fluid–crystal coexistence region of the small-ξ phase diagram has already been reviewed in section 4. Evidence for the presence of this was found in some of the earliest experiments in our model CP mixture. Immediately across the fluid–crystal coexistence boundary, homogeneous nucleation of colloidal crystal throughout the bulk of a sample was observed. Deeper into the coexistence region, however, light scattering signatures consistent with the initial stages of gas–liquid phase separation could be seen [67], although the complete two-stepped sequence of gas–liquid phase separation followed by crystallization did not occur. Even deeper into equilibrium fluid–crystal coexistence region, *transient gelation* was observed.

One of the most characteristic signatures of a sample undergoing transient gelation again comes from light scattering [67]: a ring of intensity develops in the forward direction, brightens and moves to smaller angles. After a minute or two, the collapse of this small-angle ring appears to be arrested, as are the fluctuations of the speckles on the ring. This situation persists for a finite period of time, the 'latency period' τ_{L}, and then a sudden collapse of the small-angle ring to essentially zero angle occurs, and rapid speckle fluctuations resume. (For a review of similar light scattering observations in other systems where gelation is more permanent and the ring collapse is not reported, see [86].)

Direct observation of the height of the colloid-rich portion of the sample as a function of time gave a characteristic 'inverse sigmoidal' plot. During τ_{L}, sedimentation was very slow (or even entirely absent); suddenly, however, at the same time as the collapse of the small-angle scattering ring, sedimentation would speed up by an order of magnitude until a sediment builds up and sedimentation slows down again. This phenomenon of 'delayed sedimentation' is well known in the literature for particulate or droplet dispersions with short-range attraction (see references in [87]).

Simple physical considerations would lead us to expect gelation in a system of colloids with strong, short-range attraction. Particles stick as they meet to form larger and larger ramified clusters; these clusters eventual fill space to give a gel. In the limit of infinitely deep and zero-range interparticle attraction, this is the process of 'diffusion-limited cluster aggregation' (DLCA); figure 11(a). The simplest computer model of DLCA reproduces the observed frozen small-angle scattering ring [88, 89]. The length scale associated with this peak corresponds to that of the clusters that touch to fill space. This picture is expected to apply to samples deep within the transient gelation region, with latency periods of many hours. Simulations of DLCA with finite bond strengths (particles stick on contact, but bonds can

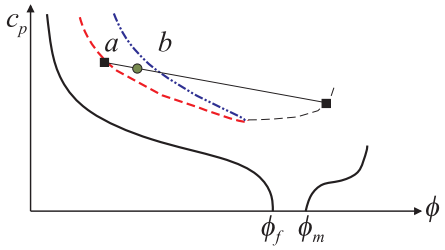

Figure 10. A schematic representation of the observations in a CP mixture with $\xi \approx 0.08$ [67]. A number of samples with $\phi < \phi_f = 0.494$ were studied. Immediately above the equilibrium fluid–crystal coexistence boundaries (bold curves), homogeneous nucleation of colloidal crystals was seen. In region (a), samples showed incipient gas–liquid phase separation, while in region (b) transient gelation was observed. The bold dashed curve is therefore taken as part of the metastable gas–liquid binodal (which is presumed to continue along the thin dashed curve), while the dot–dash curve is the gelation boundary. A sample with composition given by the dot would, as a first step towards eventual crystallization, want to undergo gas–liquid phase separation to give phases with compositions given the ends of the tie line indicated (squares). But this tie line intersects the gelation boundary, so the gas–liquid phase separation becomes arrested. In [67], where a CP mixture with $\xi \approx 0.08$ was studied, the gel boundary intersects the metastable gas–liquid binodal at $\phi \approx 0.4$.

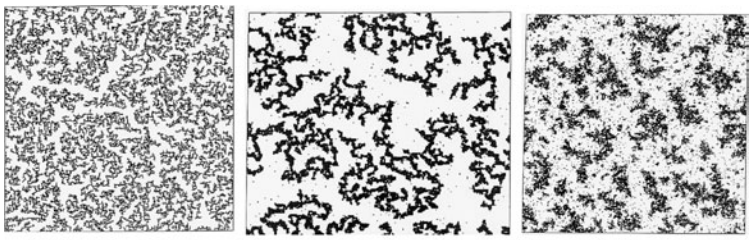

Figure 11. Simulation of diffusion-limited cluster aggregation of particles on a square lattice at area fraction 0.3 with different nearest-neighbour bond energies E. (a) $E = -\infty$ (the DLCA limit); the final stage is shown, where particles have formed a system-spanning cluster (or gel); (b) $E = -3\ k_B T$, where a system-spanning cluster (or gel) at a late stage is shown—note that the 'strands' in the spanning cluster are thicker, an indication of local restructuring; (c) at $E = -1.5\, k_B T$, no system-spanning cluster is ever formed—more or less compact clusters continue to evolve. Reproduced from [90].

break with finite probability) [90] show that the local structure can now be expected to be more compact due to rearrangements, although ramified clusters are still expected on longer length scales; these ramified cluster should again fill space, leading to gelation; figure 11(b). Real-space confocal imaging [91] provides support for this structural picture of gels in mixtures of PMMA colloids and PS. At even lower bond energies, local restructuring becomes so fast that more or less compact clusters of particles are formed; these fail to connect up to fill space; figure 11(c). The balance between thermally driven restructuring and aggregation determines the position of the gel boundary [90].

After formation, the particles gels described in the last paragraph continue to undergo restructuring. Some of the restructuring is undoubtedly driven by thermal fluctuations. In non-density-matched samples, gravity-driven solvent flow as the gel structure slowly sediments may also play a role. In these non-density-matched samples, dark-field imaging [87, 92] shows that such restructuring eventually opens up 'channels' allowing rapid back-flow of solvent, which in turn leads to large-scale breakdown of the gel structure and the onset of rapid sedimentation. A study of gels in a more complex system (charged latex + worm-like

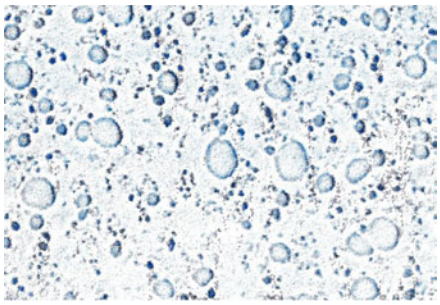

Figure 12. A low-magnification micrograph of a sample with $\xi \approx 0.08$ that completely filled its container and was tumbled slowly to simulate zero gravity. Left undisturbed, this sample would have shown transient gelation. Instead, it now gives clusters. Horizontal extent: ∼1 mm. The larger clusters are $\sim\mathcal{O}(10^2)$ particle diameters wide. Reproduced from [94].

micelle) suggests that similar physics may operate there [49]. A model has been proposed to explain why the properties of such gels, including the measured latency period τ_L, may be dependent on their shapes due to the existence of a 'stress transmission length scale' [93]. The consequence of restructuring after gelation in a density-matched sample has not yet been investigated systematically.

Consider now a sample with composition between the metastable gas–liquid binodal and the gelation boundary (region (a) in figure 10). After homogenization, thermodynamics would drive this sample to undergo gas–liquid phase separation (and thereafter, crystallization; see section 4). The putative liquid phase that develops in this process, however, will have a composition that takes it across the gelation boundary. This apparently leads to an arrest of the gas–liquid phase separation process, and gives rise to a sediment with colloid density somewhat above that of the starting, homogeneous sample but still lower than that of the putative liquid phase if gas–liquid phase separation had proceeded to completion [94, 95]. Preliminary light scattering experiments suggest that particle motion in such sediments are arrested [94]. (A similar scenario was first discussed in these terms by di Pietro and Piazza in a somewhat more complex system [96].)

Remarkably, in a density-matched experiment using the same model system, Segrè and co-workers observed long-lived clusters of particles [97]. Presumably under gravity, these clusters would sink and give rise to the sediment already described. The effect of zero averaged gravity can be achieved in a non-density-matched system if a sample completely filling a container is tumbled slowly. When this is done to a sample that otherwise would show transient gelation, and a drop of it was observed under low magnification in a microscope, clusters were also observed [94]; figure 12. In passing, note that a transient gelation sample producing clusters instead under zero average gravity suggests strongly that the position of the gel boundary is gravity dependent [86].

The detailed mechanism(s) whereby the gelation boundary actually interferes with gas–liquid phase separation remains to be worked out.

Note that since in the $\xi \sim 0.08$ system studied in [67] gas–liquid phase separation appeared always to be arrested, the gelation boundary must intersect the metastable gas–liquid binodal to the left (lower ϕ) of the critical point. This is consistent with PRISM calculations predicting that around this size ratio, the (metastable) critical point should be at $\phi \gtrsim 0.4$ [56]. If, on the other hand, the gelation boundary cuts the metastable gas–liquid binodal to the right (higher ϕ) of the critical point, then proper gas–liquid phase separation (followed by crystallization) should be possible for some samples. The metastable critical point moves to lower colloid volume fractions as ξ increases, and appears at $\phi \sim 0.2$ when it finally becomes thermodynamically stable at $\xi = \xi_c$ (cf figure 2(c)). This is presumably the main reason that we have recently observed the complete, two-stepped process of gas–liquid phase separation followed by crystallization in a system with $\xi \sim 0.2$ [36, 68] (see section 4).

The very low-density ($\phi \sim \mathcal{O}(10^{-2})$) regime of the colloidal PMMA + PS system at $\xi \sim 0.08$ has recently been studied in some detail by Lekkerkerker and co-workers [98] using confocal microscopy and small-angle light scattering [99]. Increasing the polymer concentration from zero, these authors successively observed stable single-phase fluids, nucleation of colloidal crystals, two regimes of aggregation behaviour which they labelled as 'RLCA' (reaction-limited cluster aggregation) and 'DLCA', and transient gelation at the highest polymer concentrations. In the 'RLCA' regime, there were rather compact, amorphous clusters of particles, while in the 'DLCA' regime, the clusters became ramified. It is possible that the former may correspond to what I have called arrested gas–liquid phase separation, while the latter may correspond to the cluster phase identified by Weitz and co-workers [97].

The task of predicting theoretically the position of the gel boundary has received significant recent attention. A quantitative approach is mode-coupling theory. The attractive-glass transition line that it predicts at high densities (section 5.1) continues to low densities. The significance of this mode-coupling theory line at low ϕ is, however, unclear. At this line, the theory suggests that the system drops out of equilibrium locally due to long-lived interparticle bonds. In a dense system, in particular a system that is above the percolation threshold, it is clear that this situation may lead to global non-ergodicity. The same is not true at low densities. Indeed, mode-coupling theory calculations using realistic CP mixture parameters give a transition line at low ϕ that has a significantly wrong slope compared to the experimental gel boundary [100]. Preliminary calculations suggest that a mode-coupling theory for the growing *clusters* may fit better with observations [101].

Note that comparing the non-equilibrium behaviour of different experimental CP mixtures with small ξ (or, more generally, different 'sticky-particle' systems) requires extreme care. At least four 'boundaries' of various kinds may lie 'buried' inside the equilibrium fluid–crystal coexistence region: a metastable gas–liquid binodal with its associated spinodal and a gelation boundary (which may or may not be associated with the non-ergodicity line transition predicted by mode-coupling theory); the equilibrium percolation line may also play a role. Current theoretical evidence suggests that the positions of these boundaries, both absolutely and (more importantly) relative to one another, are very sensitive functions of system and external parameters such as the range of the interparticle potential [57, 102]. Gravity almost certainly also plays a role [86]. It is therefore unsurprising that data from different experimental systems (different CP mixtures as well as other 'sticky-particle' systems, such as protein solutions) often appear to differ (or even conflict) in details. Reconciling these observations may have to await the availability of a comprehensive theoretical framework in which the role played by these (and possibly other) boundaries in controlling non-equilibrium kinetics can be discussed, at least qualitatively.

The way in which the range of non-equilibrium behaviour reviewed here influences the drying behaviour of a drop of CP mixture has recently been studied [103]. A drop with composition within the gelation boundary dries rather homogeneously, because the rigidity of the gel structure prevents flow within the droplet. Such flow occurs in drops with composition below the gelation boundary. Here, it appears that fluctuations play an important role in determining whether the drying will be essentially homogeneous or heterogeneous.

6. Summary and outlook

The system I have reviewed is a remarkably simple one: a suspension of nearly-hard-sphere colloids with added non-adsorbing, random-coil polymers that are nearly ideal. Detailed study of one experimental realization of this system over more than a decade has uncovered a range of interesting behaviour, especially in the non-equilibrium regime. The simplicity of

the experimental system has greatly facilitated comparison with theory and simulation, which in turn has led to rather detailed understanding of many of the experimental observations, although significant puzzles remain.

The increasingly complete understanding of this model system should give a good reference point for elucidating the behaviour of more complex mixtures. It also appears, however, that much of the physics revealed has generic relevance well beyond soft-condensed-matter physics. In the equilibrium realm, the study of our simple model has thrown light on the conditions needed for the existence of the liquid state itself as well as the crystallization of globular proteins. In the non-equilibrium arena, the results reviewed here have led to new understanding of how metastable minima in the free energy can control kinetic pathways and of the nature of glasses.

Many of the gaps in our knowledge of the colloidal PMMA + PS model system have already been pointed out in the main body of this review. No mention has been made so far, however, of flow and rheology. There is little doubt that the study of these topics will yield much fruit in the near future. Thus, for example, investigation of the behaviour of gels in our model system under oscillatory flow using diffusing wave echo spectroscopy and confocal microscopy is under way in Edinburgh [104]. The interfacial properties of this model system have also not been studied in any detail except for the observation of wall crystals [36, 68].

Other well-characterized CP systems exist, although knowledge of their behaviour is more limited. One of the most promising is sterically stabilized silica + random-coil PS [57] or polydimethylsiloxane (PDMS) [105, 106]. An important advantage of the silica model system is that well-characterized particles with radii down to a few nm can routinely be synthesized. This enables the detailed experimental study of a number of areas that will prove difficult using our model system (where such small particle sizes are unavailable). One obvious topic is that of interfaces. The scale of the interfacial tension between coexisting colloid gas and liquid phases is set by $k_{\mathrm{B}}T/R^2$; even with R as small as $\sim\mathcal{O}(10)$ nm, the measurements are challenging (but possible [105, 106]). Another area where small particles are needed is the study of systems with $\xi > 1$ (and, *a fortiori*, $\gg 1$) (see, e.g. [57]). Apart from its intrinsic interest, a system in which the polymers are bigger than the colloids forms an important model for some areas of biology. Finally, the use of smaller particles means that the effect of gravity can be minimized without recourse to density matching using solvent mixtures (with its concomitant complications, such as particle swelling).

In summary, it is clear that the study of simple mixtures of colloidal PMMA + random-coil PS has yielded much new physics. There is little doubt that the harvest will continue in the next few years from this and similar model systems.

Acknowledgments

The work described in this review would not have been started without Peter Pusey introducing me to the world of model colloids. Neither could the work have been done without past and present members of the soft-matter group; their names, too numerous to mention individually, will be found scattered amongst the list of references. Dr Mark Haw first suggested to me that such a review would be useful. Most of this review was completed while visiting Daan Frenkel at AMOLF, Amsterdam. I thank him for providing such a stimulating environment in which to write.

References

[1] Pusey P N and van Megen W 1986 *Nature* **320** 340

[2] Pusey P N, van Megen W, Bartlett P, Ackerson B J, Rarity J G and Underwood S M 1989 *Phys. Rev. Lett.* **63** 2753

[3] Frenkel D and Ladd A J C 1984 *J. Chem. Phys.* **81** 3188
[4] Bruce A D, Jackson A N, Ackland G J and Wilding N B 2000 *Phys. Rev.* E **61** 906
[5] van Megen W, Underwood S M and Pusey P N 1991 *J. Chem. Soc. Faraday Trans.* **87** 395
[6] Pusey P N and van Megen W 1987 *Phys. Rev. Lett.* **59** 2083
[7] Bengtzelius U, Götze W and Sjölander A 1984 *J. Physique Coll.* **17** 5915
[8] Bartlett P, Ottewill R H and Pusey P N 1990 *J. Chem. Phys.* **93** 1299
[9] Eldridge M D, Madden P A, Pusey P N and Bartlett P 1995 *Mol. Phys.* **84** 395
[10] Pusey P N 1991 *Liquids, Freezing and the Glass Transition* ed J-P Hansen, D Levesque and J Zinn-Justin (Amsterdam: Elsevier) ch 10
[11] Haw M D 2002 *J. Phys.: Condens. Matter* **14 7769**
[12] Asakura S and Oosawa F 1954 *J. Chem. Phys.* **22** 1255
[13] Vrij A 1976 *Pure Appl. Chem.* **48** 471
[14] Gast A P, Russel W B and Hall C K 1986 *J. Colloid Interface Sci.* **109** 161
[15] Sperry P R 1984 *J. Colloid Interface Sci.* **99** 97
[16] Piazza R, Iacopini S, Pierno M and Vignati E 2002 *J. Phys.: Condens. Matter* **14 7563**
[17] Poon W C K 1998 *Curr. Opin. Colloid Interface Sci.* **3** 593
[18] Antl L, Hill R D, Ottewill R H, Owens S M, Papworth S and Waters J A 1986 *Colloids Surf.* **17** 67
[19] Underwood S M, Taylor J R and van Megen W 1994 *Langmuir* **10** 3550
[20] Golz P M 1999 Dynamics of colloids in polymer solutions *PhD Thesis* University of Edinburgh
[21] Castello B A de L, Luckham P F and Tadros Th F 1992 *Langmuir* **8** 464
[22] Auer S and Frenkel D 2002 *J. Phys.: Condens. Matter* **14 7667**
[23] Berry C G 1966 *J. Chem. Phys.* **44** 1550
[24] Poon W C K, Selfe J S, Robertson M B, Ilett S M, Pirie A D and Pusey P N 1993 *J. Physique* II **3** 1075
[25] Bartlett P and Henderson S 2002 *J. Phys.: Condens. Matter* **14 7757**
[26] Rudhart D, Bechinger C and Leiderer P *Phys. Rev. Lett.* **81** 1330
[27] Starrs L and Bartlett P 2003 *Faraday Discuss.* **123** at press
[28] Ilett S M, Orrock A, Poon W C K and Pusey P N 1995 *Phys. Rev.* E **51** 1344
[29] Lekkerkerker H N W, Poon W C K, Pusey P N, Stroobants A and Warren P B 1992 *Europhys. Lett.* **20** 559
[30] Moussaïd A, Poon W C K, Pusey P N and Soliva M F 1999 *Phys. Rev. Lett.* **82** 225
[31] Widom B 1967 *Science* **157** 375
[32] Lindemann F A 1910 *Z. Phys.* **11** 609
[33] Hagen M H J and Frenkel D 1994 *J. Chem. Phys.* **101** 4093
[34] Poon W C K 1997 *Phys. Rev.* E **55** 3762
[35] Warren P B, Ilett S M and Poon W C K 1995 *Phys. Rev.* E **52** 5205
[36] Martelozzo V 2001 Crystallization and phase separation in colloidal suspensions *PhD Thesis* University of Edinburgh
[37] Jusufi A, Watzlawek M and Löwen H 1999 *Macromolecules* **32** 4470
[38] von Ferber C, Holovatch Y, Jusufi A, Likos C N, Löwen H and Watzlawek M 2001 *J. Mol. Liq.* **93** 151
[39] Poon W C K, Egelhaaf S U, Stellbrink J, Allgaier J, Schofield A B and Pusey P N 2001 *Proc. R. Soc.* A **359** 897
[40] Pusey P N 1987 *J. Physique* **48** 709
[41] Fairhurst D J 1999 Polydispersity in colloidal phase separation *PhD thesis* University of Edinburgh
[42] Fairhurst D J, Pham K N and Poon W C K, in preparation
[43] Sollich P 2002 *J. Phys.: Condens. Matter* **14** R79
[44] Evans R M L, Fairhurst D J and Poon W C K 1998 *Phys. Rev. Lett.* **81** 1326
[45] Evans R M L 2001 *J. Chem. Phys.* **114** 1915
[46] Xu H and Baus M 2000 *Phys. Rev.* E **61** 3249
[47] Warren P B 1997 *Langmuir* **13** 4588
[48] Sear R P and Frenkel D 1997 *Phys. Rev.* E **55** 1677
[49] Petekidis G, Galloway L A, Egelhaaf S U, Cates M E and Poon W C K 2002 *Langmuir* **18** 4248
[50] Galloway L A, Warren P B, Fuchs M, Egelhaaf S U and Poon W C K, in preparation
[51] Segrè P N, van Megen W, Pusey P N, Schätzel K and Peters W 1995 *J. Mod. Opt.* **42** 1929
[52] Meijer E J and Frenkel D 1994 *J. Chem. Phys.* **100** 6873
[53] Louis A A, Finken R and Hansen J-P 1999 *Europhys. Lett.* **46** 741
[54] Dijkstra M, Brader J M and Evans R 1999 *J. Phys.: Condens. Matter* **11** 10079
[55] Bolhuis P G, Louis A A and Hansen J-P 2002 *Preprint* cond-mat/0206061
[56] Fuchs M and Schweizer K S 2002 *J. Phys.: Condens. Matter* **14** R239
[57] Ramakrishnan S, Fuchs M, Schweizer K S and Zukoski C F 2002 *J. Chem. Phys.* **116** 2201

[58] Aarts D G A L, Tuinier R and Lekkerkerker H N W 2002 *J. Phys.: Condens. Matter* **14 7551**
[59] Leal Calderon F, Bibette J and Biais J 1993 *Europhys. Lett.* **23** 653
[60] Renth F, Poon W C K and Evans R M L 2001 *Phys. Rev. Lett.* **64** 031402
[61] Poon W C K *Soft and Fragile Matter: Non-Equilibrium Dynamics, Metastability and Flow* ed M E Cates and R M Evans (Bristol: Institute of Physics Publishing) ch 1
[62] Harland J L and van Megen W 1997 *Phys. Rev.* E **55** 3054
[63] Elliot M S, Haddon S B and Poon W C K 2001 *J. Phys.: Condens. Matter* **13** L553
[64] Gasser U, Weeks E R, Schofield A B, Pusey P N and Weitz D A 2001 *Science* **292** 258
[65] Auer S and Frenkel D 2001 *Nature* **409** 1020
[66] Wu D T 1997 *Solid State Phys.* **50** 37
[67] Poon W C K, Pirie A D and Pusey P N 1995 *Faraday Discuss.* **101** 65
[68] Martelozzo V, Pusey P N and Poon W C K 2002 in preparation
[69] Ostwald J 1897 *Z. Phys. Chem.* **22** 286
[70] Hobbie E K 1999 *Langmuir* **15** 8807
[71] Evans R M L, Poon W C K and Cates M E 1997 *Europhys. Lett.* **38** 595
[72] Evans R M L and Cates M E 1997 *Phys. Rev.* E **56** 5738
[73] Evans R M L and Poon W C K 1997 *Phys. Rev.* E **56** 5748
[74] Cahn J W 1969 *J. Am. Ceram. Soc.* **52** 118
[75] Evans R M L, Poon W C K and Renth R 2001 *Phys. Rev.* E **64** 031403
[76] Poon W C K, Renth F and Evans R M L 2000 *J. Phys.: Condens. Matter* **12** A269
[77] ten Wolde P R and Frenkel D 1997 *Science* **277** 1975
[78] van Megen W and Underwood S M 1993 *Phys. Rev.* E **47** 248
[79] Pham K N, Puertas A M, Bergenholtz J, Egelhaaf S U, Moussaïd A, Pusey P N, Schofield A B, Cates M E, Fuchs M and Poon W C K 2002 *Science* **296** 104
[80] Campbell A I and Bartlett P 2002 *J. Colloid Interface Sci.* submitted
[81] Richert R 2002 *J. Phys.: Condens. Matter* **14** R703
[82] Weeks E R, Crocker J C, Levitt A C, Schofield A and Weitz D A 2000 *Science* **287** 627
[83] Dawson K, Foffi G, Fuchs M, Götze W, Sciortino F, Sperl M, Tartaglia P, Voigtmann Th and Zaccarelli G 2001 *Phys. Rev.* E **63** 011401
[84] Lettinga M P, van Zandvoort M A M J, van Kats C M and Philipse A P 2000 *Langmuir* **16** 6156
[85] Ferrer M L, Lawrence C, Dernirjian B G, Kivelson D, Alba-Simionesco C and Tarjus G 1998 *J. Chem. Phys.* **109** 8010
[86] Poon W C K and Haw M D 1997 *Adv. Colloid Interface Sci.* **73** 71
[87] Poon W C K, Starrs L, Meeker S P, Moussaïd, Evans R M L, Pusey P N and Robins M M 1999 *Faraday Discuss.* **112** 143
[88] Haw M D, Poon W C K and Pusey P N 1994 *Physica* A **208** 8
[89] Haw M D, Sievwright M, Poon W C K and Pusey P N 1995 *Physica* A **217** 231
[90] Haw M D, Sievwright M, Poon W C K and Pusey P N 1995 *Adv. Colloid Interface Sci.* **62** 1
[91] Dinsmore A D and Weitz D A 2002 *J. Phys.: Condens. Matter* **14 7581**
[92] Starrs L, Poon W C K, Hibberd D and Robins M M 2002 *J. Phys.: Condens. Matter* **14** 2485
[93] Evans R M L and Starrs L 2002 *J. Phys.: Condens. Matter* **14** 2507
[94] Pirie A D 1995 A light scattering study of colloid–polymer mixtures *PhD Thesis* University of Edinburgh
[95] Meeker S P 1998 Low-shear rheology and delayed sedimentation of colloidal systems *PhD Thesis* University of Edinburgh
[96] Piazza R and di Pietro G 1994 *Europhys. Lett.* **28** 445
[97] Segrè P N, Prasad V, Schofield A B and Weitz D A 2001 *Phys. Rev. Lett.* **86** 6042
[98] de Hoog E H A, Kegel W K, van Blaaderen A and Lekkerkerker H N W 2001 *Phys. Rev.* E **64** 021407
[99] Anderson V J, de Hoog E H A and Lekkerkerker H N W 2001 *Phys. Rev.* E **65** 011403
[100] Bergenholtz J, Pham K N, Poon W C K and Fuchs M, in preparation
[101] Kroy K, Cates M E and Poon W C K, in preparation
[102] Noro M G, Kern N and Frenkel D 1999 *Europhys. Lett.* **48** 332
[103] Haw M D, Gillie M and Poon W C K 2002 *Langmuir* **18** 1626
[104] Smith P A, Petekidis G, Egelhaaf S U, Poon W C K and Pusey P N, in preparation
[105] de Hoog E H A and Lekkerkerker H N W 1999 *J. Phys. Chem.* B **103** 5274
[106] de Hoog E H A, Lekkerkerker H N W, Schulz J and Findenegg G H 1999 *J. Phys. Chem.* B **103** 10 657